J.Fluid Mech. (1997), vol. 351, *pp.* 289-300.

Bubbles rising in line: why is the first approximation so bad?

By J.F. Harper

School of Mathematical and Computing Sciences,
Victoria University, Wellington, New Zealand

(Received 3 December 1996 and in revised form 24 June 1997)

An analytical theory is given for the viscous wake behind a spherical bubble rising steadily in a pure liquid at high Reynolds number, and for that wake's effect on the motion of a second bubble rising underneath the first. Previous theoretical work on this subject consists of just two papers: a first approximation ignoring wake vorticity diffusion between the bubbles, and a full numerical solution avoiding simplifying approximations (apart from that of spherical shape of the bubbles). A second approximation is now found; it removes much of the discrepancy between the first approximation and the full solution. The leading-order calculation of wake vorticity diffusion uses a transformation of the independent variables which appears to be new. Experimental work to date has disagreed with all the theoretical work, but it addresses a somewhat different problem: a line of many bubbles.

1 Introduction

If a single spherical gas bubble of radius a rises steadily at speed U in a pure liquid at a large Reynolds number $R = 2Ua/\nu$, where ν is the kinematic viscosity of the liquid, there is a fairly simple theory due to Moore (1963) which describes the flow to a good

approximation, with a weak viscous boundary layer around the bubble surface merging into an irrotational flow at a distance, and with a wake behind (and beneath) the bubble in which vorticity diffusion may be neglected except over vertical distances much larger than the bubble radius. That vorticity diffusion has not hitherto been calculated except for distances below the bubble much larger than $aR^{1/2}$ where the usual wake similarity solution applies (Rosenhead 1963 p. 455–456). One of the aims of this paper is to give the solution much nearer the bubble (distances of order a). If the surface tension is large enough, one can ignore the distortions from spherical shape that were first calculated by Moore (1965). The boundary layer can be described as weak because the velocity everywhere is close to its irrotational value, and velocity derivatives are different from the irrotational ones by amounts of their own order. This contrasts with the more familiar case of boundary layers on rigid surfaces, where velocity perturbations are of the order of the irrotational velocity, and velocity derivatives are large.

There has long been experimental evidence (summarised by Harper 1972, herein called H72), that Moore's model of the flow is a good one for a single bubble if R is of order 100 or more; recent work (e.g. Duineveld 1995, Maxworthy et al. 1996) has confirmed it. There is also evidence for Moore's result from Navier-Stokes numerical solutions, without physical simplifying approximations such as inviscid regions and boundary layers, due to Brabston & Keller (1975), Ryskin & Leal (1984a,b), Dandy & Leal (1986), Magnaudet et al. (1995), and Blanco & Magnaudet (1995). Unfortunately the last two papers also found worrying discrepancies with some of the earlier work, not all of which they could explain. It seems that Navier-Stokes computation with tangentially stress-free boundaries poses some numerical difficulties that are not yet entirely understood. Hence analytical work on more problems of this kind seems called for. The approach in this paper is to study a vertical line of two bubbles, as far as possible analytically, and try to avoid numerical errors by using software (NAG 1995) only for well-understood tasks: quadrature and evaluating special functions (erf, erfc, and Bessel I_n, J_n). If this approach succeeds, it also increases physical understanding of the different mechanisms involved.

Vertical lines of rising bubbles are often seen in glasses of various drinks, e.g. lemonade, lager, or champagne. Their lateral stability was explained by Harper (1970b), herein called H70b, for high values of R, and by Harper (1983) and Lerner & Harper (1991) in the Stokes limit $R \to 0$. Lateral stability is due to surface activity, which can achieve this effect even

if the amount of impurity is too small to appreciably affect the speed of rise. (H70b showed that in the total absence of surface activity a vertical line would be unstable, by a method that does not depend on the Reynolds number being large, though it would not be valid in the Stokes limit.)

Vertical stability is a more difficult problem, even when surface activity is small enough to be negligible apart from causing lateral stability, which is assumed throughout what follows. H70b extended Moore's (1963) theory of the flow at large R to the case of a pair of spherical bubbles of the same size rising in quiescent liquid in the same line, assuming that vorticity diffusion between the bubbles was negligible but allowing for its effect in the boundary layers around the bubbles. Yuan & Prosperetti (1994), herein called YP, treated the same problem by computing the flow using the full Navier-Stokes equations, avoiding the approximation of large R. YP found some differences between their results and those of H70b, which seem to be largely due to error terms in the latter paper not being negligibly small. Katz & Meneveau (1996) (herein called KM) did experiments whose most striking feature was that the second in a line of many equally spaced bubbles rose faster than the first or third, then the fourth rose faster than the third, and the resulting close pairs coalesced, all the way down the line. This pairing-off process is not predicted by either YP, H70b or the present paper; they all consider only two bubbles. Harper (1983) predicted pairing-off theoretically in the Stokes limit for three or more bubbles, though not for two. There seems little hope of any advance on KM's semi-empirical theory for three or more bubbles at finite R until the wake between bubbles is studied in much more detail than even the present work attempts.

The drag coefficients C_{D1}, C_{D2} found by H70b for the top and bottom bubbles respectively (when only two are present) are

$$C_{D1} = \frac{48}{R}\left(1 - \frac{2.211\ldots}{R^{1/2}}\right) - 12s^4 + O(s^6) + O(R^{-11/6}) + O(R^{-2}s^{-1}), \tag{1}$$

$$C_{D2} = \frac{48}{R}\left(1 - \frac{4.345\ldots}{R^{1/2}}\right) + 12s^4 + O(s^6) + O(R^{-11/6}) + O(R^{-2}s^{-1}), \tag{2}$$

where the flow is assumed at least quasi-steady, the drag force is $\frac{1}{2}\pi a^2 \rho U^2 C_D$ as usual, ρ is the liquid density, assumed much larger than the gas density, R is the Reynolds number based on the bubble diameter, and s is the ratio of bubble radius to distance between the bubble centres, so that $s = \frac{1}{2}$ for bubbles in contact, and physically possible bubbles have $0 < s < \frac{1}{2}$. H70b used a small-s expansion throughout, in which the speed v_θ of the fluid

at the surface of the first bubble is

$$v_\theta = \tfrac{3}{2}U \sin\theta\{1 - s^3 + 5s^4 \cos\theta + \tfrac{1}{2}s^5(7 + 35\cos^2\theta) + O(s^6)\}, \tag{3}$$

where the spherical polar angle $\theta = 0$ at the top stagnation point. Equation (3) implies that a term ΔC_D should be added to the right-hand sides of (1) and (2), where

$$\Delta C_D = \frac{48}{R}\{-2s^3 + 14s^5 + O(s^6)\}, \tag{4}$$

because Harper (1970a, 1971) found the viscous dissipation rate E of the irrotational flow of a uniform stream of dynamic viscosity η past a fixed surface S as

$$E = 2\eta \int\int_S \frac{1}{h_1}\left(v_2^2 h_3 \frac{\partial h_2}{\partial q_1} + v_3^2 h_2 \frac{\partial h_3}{\partial q_1}\right) dq_2 dq_3. \tag{5}$$

In (5), (q_1, q_2, q_3) are orthogonal coordinates, S is a surface $q_1 =$ constant, and $h_i = \sqrt{g_{ii}}$, where g_{ii} is a diagonal metric coefficient, $i = 1, 2, 3$, and the Einstein summation convention is not used.

It is convenient to define a dimensionless bubble separation $d = 1/s$; note that YP defined their d as the present d multiplied by the bubble radius. YP concentrated on the viscous contributions to C_{Dn} for $n = 1, 2$. So shall I, by defining C_{Vn} to be those terms in C_{Dn} that depend on R: all except $\pm 12s^4 + O(s^6)$ in (1), (2) and (3). Because

$$C_{Vn} = 48/R + O(s^3 R^{-1}) + O(R^{-3/2}) + O(R^{-2}s^{-1}), \tag{6}$$

YP defined drag functions F_n which tend to non-zero values as $R \to \infty$ by

$$F_n = R^{1/2}(1 - \frac{RC_{Vn}}{48}). \tag{7}$$

Equations (1) and (2) are asymptotically valid and the terms used by H70b are the dominant ones if $R \gg 1$ and $s \ll 1$, provided that $R^{-3/2} \gg R^{-2}s^{-1}$, i.e. $R^{-1/2}d \ll 1$. Unfortunately for the practical utility of the theory, that last condition (which comes from the neglect of viscous forces in the wake between the bubbles) is seldom satisfied for real bubbles; a typical real situation might have $R = 100$ and $d = 10$, which gives $R^{-1/2}d = 1$. It is therefore no surprise that YP found that (1) and (2), and the vorticity calculations on which they were based, were good approximations only for R so high that the bubbles could not be nearly spherical in any possible real fluid.

***** Figure 1 near here *****

Figure 1, which was redrawn from Figure 4 of YP, reveals this. It plots the results of YP and H70b for the dimensionless wake vorticity $\omega a/U$ along the abscissa, in terms of dimensionless cylindrical polar radius m/a along the ordinate. The graphs are for $d = 8$ and for three different Reynolds numbers (100, 200, 500), at three different positions in the wake between the bubbles. These positions were given by YP as (a) 0.16 bubble radii above the top of the lower bubble, (b) halfway between the bubbles, and (c) 0.16 radii below the bottom of the upper bubble, but Dr Yuan (personal communication, 1996) has said that that 0.16 should have been given as 0.12.

A question that naturally arises is whether one can significantly improve on H70b and obtain most of YP's answer with a small fraction of their work, by allowing for viscosity in the wake between the bubbles and finding the coefficient of $R^{-1/2}d$. This paper is an attempt to answer that question and improve physical understanding of the whole problem. A feature of the method is a transformation of the governing equation to a simple canonical form which appears to be new, and which simplifies the process of finding the vorticity distribution in the wake from the vorticity distribution at its upstream end, which is the rear of the first bubble. The other methods employed are not new, being in Rosenhead (1963), H70b, H72, and NAG (1995).

YP also dealt with some unsteady flows, but those are not discussed here. Throughout the present work the flow will be assumed to behave as if it were steady, even though s will change slowly for bubbles of equal size whenever $C_{D1} \neq C_{D2}$, and so the flow pattern will change slowly. Non-sphericity of bubbles also affects their slow relative velocity. That complication will be ignored here, although both YP and KM suggested that it might explain the discrepancy between their theory and experiments. As that discrepancy could be of order 10% for bubbles whose ellipticity was far smaller than 10%, the cause must be sought elsewhere. It seems unlikely to be surface activity, at least at the higher Reynolds numbers used by KM, because of the closeness between their drag coefficients and the theory for pure liquids. The most likely cause is that finding the drag coefficient of the second (or subsequent) bubble gives its velocity relative to the fluid in which it finds itself, which is already rising because it is in the wake of the bubble(s) above. KM gave an approximate theory of this effect in the asymptotic wake far below a bubble and showed that the additional velocity is of order $R^{-1}U$. This is equivalent to reducing C_{D2} by an amount of order $R^{-1}C_{D2}$ or $O(R^{-2})$, which is negligible here because other error terms are

larger. The present treatment is used in Section 5 below to show that KM's result can be extended to the wake much nearer the first bubble than they thought, but that an infinite line of bubbles is not a well-posed problem.

2 The first bubble: leading-order theory

It is easiest to use a frame of reference moving with the bubbles; the first bubble being vertically above the second, and the whole configuration being axially symmetric. Instability, surface activity, and deformation of the bubbles from spherical shape will be ignored; these are good approximations in pure liquids with low values of $M = g\eta^4/\rho\sigma^3$ if the Weber number W given by

$$W = \frac{2\rho U^2 a}{\sigma} = \left(\frac{4MR^4}{3C_D}\right)^{1/3} \ll 1, \tag{8}$$

the drag coefficient C_D being defined as usual, as the drag force on the bubble divided by $\frac{1}{2}\rho U^2 \pi a^2$; see, for example, H72. Here ρ is the liquid density, assumed much larger than the gas density, and $\eta = \rho\nu$ is the liquid dynamic viscosity, assumed much larger than the gas dynamic viscosity. Because C_D is not far from $48/R$, (Levich 1949, and 1, 2, 4 above), and there are few fluids apart from liquid metals and hydrogen with $M < 10^{-11}$ and none apart from superfluid helium with $M < 10^{-14}$, R can be a few hundred at most if the approximations are to be valid. This paper deals only with the case $R \gg 1$.

Let Ω be the dimensionless circulation density $(a^2/U)(\omega/m)$, as in H72. In the boundary layer around the first bubble let $\Omega = \Omega_1$. In spherical polar coordinates (r, θ) such that the bubble surface is $r = a$ and the direction $\theta = 0$ points upstream, it is known (H70b) that if Ψ is the irrotational approximation to the stream function, $\mu = \cos\theta$, the θ component of velocity is v_θ, and terms $O(s^3)$ are neglected, then

$$v_\theta = \tfrac{3}{2}U \sin\theta + UR^{-1/2} f_1(x, z) \operatorname{cosec}\theta, \tag{9}$$

$$x = \tfrac{1}{4}(2 - 3\mu + \mu^3) = \tfrac{1}{4}(1 - \mu)^2(2 + \mu), \tag{10}$$

$$z = \frac{3R^{1/2}(r - a)\sin^2\theta}{8a} = \frac{R^{1/2}\Psi}{4Ua^2}, \tag{11}$$

where f_1 is dimensionless and determines the velocity perturbation from the irrotational value, $f_1 = O(1)$ and $z = O(1)$ in the boundary layer, and x increases from 0 to 1 as the fluid travels around the bubble. To a first approximation, Ω_1 is related to f_1 by

$$f_1(x, z) = -\frac{8}{3}\int_z^\infty \Omega_1(x, t)\, dt. \tag{12}$$

Then $\Omega_1(x,z)$ and $f_1(x,z)$ obey the same diffusion equation

$$\frac{\partial^2 y}{\partial z^2} = 4\frac{\partial y}{\partial x}, \tag{13}$$

with boundary conditions

$$\Omega_1(0,z) = 0, \quad \Omega_1(x,0) = 3, \tag{14}$$

$$f_1(0,z) = 0, \quad \frac{\partial f_1}{\partial z}(x,0) = 8. \tag{15}$$

The solutions are immediate (Carslaw & Jaeger 1959, H70b):

$$\Omega_1(x,z) = 3\,\mathrm{erfc}(zx^{-1/2}), \quad f_1(x,z) = -8x^{1/2}\,\mathrm{ierfc}(zx^{-1/2}). \tag{16}$$

3 The first bubble: second-order theory

Section 2 recapitulated briefly the relevant parts of H70b, but a better approximation to the second equation in (14) and (15) is now needed. Those equations derive from the surface boundary condition of vanishing shear stress τ. With error $o(R^{-1/2})$, $\tau = 0$ implies that

$$\frac{\partial f_1}{\partial z}(x,0) = 8 + \frac{8R^{-1/2} f_1(x,0)}{3\sin^2\theta}, \tag{17}$$

and the definition of vorticity and the continuity equation then give

$$\Omega_1(x,0) = 3 + \frac{2R^{-1/2} f_1(x,0)}{\sin^2\theta} = 3 + \frac{2u}{\sin\theta} = 3 + \Omega_{S1}(x,0), \text{ say,} \tag{18}$$

where Uu is the perturbation of tangential velocity from its irrotational value. Equation (18) then shows that the leading contribution to the correction term Ω_{S1} comes from the rear stagnation region where

$$\Omega_{S1}(x,0) = -\frac{6R^{-1/6}}{m_1}\int_0^\infty\int_0^\infty\int_0^\infty p^2 q e^{-qr} J_1(pq) J_1(m_1 q)\,\mathrm{erfc}(\tfrac{3}{8}p^2 r)\,dpdqdr, \tag{19}$$

by H72 equation (2.39), if

$$m_1 = \frac{mR^{1/6}}{a} \sim R^{1/6}\sin\theta \sim 2R^{1/6}\left(\frac{1-x}{3}\right)^{1/4}, \tag{20}$$

so that $m_1 = O(1)$ in the stagnation region, where $\Omega_2 = O(R^{-1/6})$, rather than the much smaller $\Omega_2 = O(R^{-1/2})$ which holds over most of the bubble's surface.

Equation (19) is somewhat tedious for numerical evaluation, but as Ω_{S1} is a small correction its asymptotic forms for small and large m_1 can be used instead without serious error. These forms are (Harper & Moore 1968, H72)

$$\Omega_{S1}(x,0) \sim -\frac{8\Gamma(\frac{5}{6})\Gamma(\frac{2}{3})^2}{3^{1/3}\pi}R^{-1/6} = -\alpha R^{-1/6} \text{ if } m_1 \ll 1, \tag{21}$$

where $\alpha = 3.654$ to four figures, and

$$\Omega_{S1}(x,0) \sim -\frac{16R^{-1/2}}{\pi^{1/2}(\pi-\theta)^2} \sim -\frac{\beta R^{-1/2}}{(1-x)^{1/2}} \sim -\frac{16R^{-1/6}}{\pi^{1/2}m_1^2} \text{ if } m_1 \gg 1, \tag{22}$$

where $\beta = 4(3/\pi)^{1/2} = 3.909$ to four figures. Let us approximate to $\Omega_2(x,0)$ by (21) or (22) according as $m_1 < c$ or $m_1 > c$, where c is chosen to make the two expressions equal at $m_1 = c$. Let $x = x_0$ where $m_1 = c$, and define γ by

$$\gamma = (1-x_0)^{-1/2} = \frac{4R^{1/3}}{3^{1/2}c^2} = \frac{\alpha R^{1/3}}{\beta}. \tag{23}$$

The solution of (13) with boundary conditions (22) and $\Omega_{S1}(0,z) = 0$ is

$$\Omega_{S1}(x,z) \sim \frac{\alpha R^{-1/6}}{\gamma(1-x)^{1/2}} \exp\left(\frac{z^2}{1-x}\right) \operatorname{erfc}\left(\frac{z}{x^{1/2}[1-x]^{1/2}}\right) \text{ if } x < x_0. \tag{24}$$

For $x_0 < x < 1$ the boundary conditions are

$$\Omega_{S1}(x,0) = -\alpha R^{-1/6}, \tag{25}$$

$$\Omega_{S1}(1-\gamma,z) = -\alpha R^{-1/6}\exp(\gamma^2 z^2)\operatorname{erfc}(\gamma z x_0^{-1/2}), \tag{26}$$

from (22) and (24), and simple diffusion theory then gives Ω_{S1} at the bottom of the first bubble as

$$\Omega_{S1}(1,z) = -\alpha R^{-1/6}\left\{\operatorname{erfc}(\gamma z) + \frac{\exp(-\delta^2 z^2) - \exp(-\gamma^2 z^2)}{\pi^{1/2}\gamma z}\right\}, \tag{27}$$

where

$$\delta^2 = 2 - 1/\gamma^2 = 2 - O(R^{-2/3}).$$

As one would have expected from (25), (26), $\Omega_{S1} = O(R^{-1/6})$ for all $z > 0$. It is because $R^{-1/6}$ is not really small in practice that Ω_{S1} needs to be considered at all; even $500^{-1/6} = 0.355$. Various terms of order $R^{-1/2}$ have been neglected in the above theory; this should be borne in mind when assessing how well the results agree with YP.

4 The wake between the bubbles

As the fluid travels past the bottom stagnation point on the first bubble, circulation density remains constant along each streamline to a first approximation, i.e. Ω remains the same function of Ψ that it was at the rear of the first bubble. Accordingly, let $\Omega_W = (a^2/U)(\omega/m)$ be the dimensionless circulation density in the wake between the bubbles, and then the boundary condition at the upstream end is, to a first approximation,

$$\Omega_W = 3\,\mathrm{erfc}\, z + \Omega_{S1}(1, z) = \Omega_1(1, z), \tag{28}$$

where Ω_{S1} is given by (27).

The wake thickness is $O(aR^{-1/4}) \ll a$ if $R \gg 1$, and the boundary-layer equation obeyed by Ω_W in the wake is readily deduced from the vorticity equation as

$$\frac{\partial \Omega_W}{\partial w} = z\frac{\partial^2 \Omega_W}{\partial z^2} + 2\frac{\partial \Omega_W}{\partial z}, \tag{29}$$

where $z = R^{1/2}\Psi/(4Ua^2)$ as before, $w = X/(aR^{1/2})$, and X is the distance downstream from the rear stagnation point on the first bubble, so that $0 < w < R^{-1/2}(d-2)$ in the wake. The variables w, z permit solutions of (29) to be found readily, and they work because the velocity is close to its irrotational value throughout this wake. In spite of its simplicity, (29) appears to be new, though it is of course a generalisation, to a non-uniform but still axially symmetric stream, of the cylindrical polar coordinates usually used for wakes (see, for example, Rosenhead 1963 Section VIII.18). The boundary conditions for (29) are (28) and the condition that

$$\Omega_W(w, z) \text{ remains finite as } z \to 0. \tag{30}$$

The variables are separable in (29), and an exact solution is $e^{-\lambda w} J_1(2[\lambda z]^{1/2}) z^{-1/2}$. The other solution involving the Bessel function Y_1 is discarded because it does not obey (30). One must have λ real and positive to avoid solutions tending to infinity for large w or z. The solution of (28), (29), (30) can be found from the Hankel transform in the Bateman Manuscript Project (1954) and from Gradshteyn & Ryzhik (1980) equation (6.633.2) as

$$\begin{aligned}\Omega_W(w, z) &= \frac{2\exp(-z/w)}{wz^{1/2}} \int_0^\infty t^2 \Omega_1(1, t^2) \exp(-t^2/w) I_1\left(\frac{2tz^{1/2}}{w}\right) dt \\ &= \frac{2}{wz^{1/2}} \int_0^\infty t^2 \Omega_1(1, t^2) \exp\left(-\frac{[t - z^{1/2}]^2}{w}\right) I_{1e}\left(\frac{2tz^{1/2}}{w}\right) dt,\end{aligned} \tag{31}$$

where the function $I_{1e}(x) = I_1(x)e^{-|x|}$ is the function S18CFF of the NAG (1995) software. The integral (31) converges for all positive w and z because $0 < I_{1e}(x) < 1$ for all $x > 0$. It has an asymptotic but not convergent series in ascending powers of w, and a convergent series in ascending powers of w^{-1}. Equation (31) agrees with the well-known far wake solution in Rosenhead (1963) Section VIII.18, because the leading-order approximation to C_D for large d is $48/R$.

Although the integral (31) has to be evaluated numerically in general, its value on the axis of symmetry can be found analytically as

$$\Omega_W(w,0) = 3e_2(w) - \alpha R^{-1/6}\left\{e_2(\gamma w) - (\delta/\gamma)e_1(\delta w) + e_1(\gamma w)\right\}, \tag{32}$$

where

$$e_1(w) = \frac{1}{2w^2}\,\mathrm{erfc}\,\frac{1}{2w}\,\exp\frac{1}{4w^2},$$
$$e_2(w) = 1 - \frac{1}{\pi^{1/2}w} + (1-2w^2)e_1(w).$$

***** Figures 2, 3 near here *****

Figure 2 shows $\omega a/U$ as a function of m across the wake, calculated by numerically integrating (31) without the second-order theory of Section 3 which gave the $O(R^{-1/6})$ contributions to Ω_W. It compares quite well with the YP results in Figure 1 except near the first bubble (see Figures 1c, 2c). Figure 3 includes the second-order theory. Its vorticity distributions are seen to be even nearer those of YP, especially near the first bubble, but further down the wake there is less difference, because vorticity diffusion in the wake smears out the second-order terms more rapidly away from the stagnation point, as those terms (27) vary more rapidly with z than the first-order term (16) does.

5 The drag on the second bubble

***** Figure 4 near here *****

Figure 4 was redrawn from YP Figure 3, and it shows that Moore's (1963) result $F_1 = 2.211$ for the drag perturbation on the first bubble (7) is close to the truth, except for small d. This means that the second-order terms of Section 3 have little effect on the first bubble, and that the analogous terms at the second bubble's stagnation points should have little effect on its drag. One would expect, however, that because the first bubble's

second-order terms do have a noticeable effect on the wake between the bubbles, they should affect the value of the second bubble's drag through the value of F_2. It is therefore worth investigating the boundary layer around the second bubble.

The second bubble's boundary layer is very like the first. If r_2, θ_2 are spherical polar coordinates centred on this bubble, but now $\mu_2 = \cos\theta_2$, $x_2 = \frac{1}{4}(2+\mu_2)(1-\mu_2)^2$, so that $0 \le x_2 \le 1$, and $\Omega = \Omega_2(x_2, z)$, $f_2 = -(8/3)\int_z^\infty \Omega_2(x_2, z)\, dz$, one finds that Ω_2 and f_2 still obey (13), while (14) becomes

$$\Omega_2(1, z) = \Omega_W\left(R^{-1/2}[d-2], z\right) = F(z), \text{ say.} \tag{33}$$

Stagnation-point corrections need not be taken into account here: they affect the drag coefficient C_{D2} only by terms of smaller order than those we do take into account.

Green's functions may now be used to find f_2 and Ω_2 (Carslaw & Jaeger 1959); after integrations by parts to improve the numerical accuracy (by removing all inverse powers of $x_2^{1/2}$ except in the arguments of error functions), the results that will be needed later for $0 \le x_2 \le 1$ are, if one puts $\xi = {x_2}^{1/2}$ for brevity,

$$f2(x_2, 0) = -\frac{8\xi}{\pi^{1/2}} - \frac{8}{3}\int_0^\infty F(t)\,\mathrm{erf}\,\frac{t}{\xi}\, dt, \tag{34}$$

$$\frac{\partial f_2}{\partial z}(x_2, z) = 8\,\mathrm{erfc}\,\frac{z}{\xi} + c\,\mathrm{erf}\,\frac{z}{\xi} + \frac{4}{3}\int_0^\infty \frac{dF(t)}{dt}\left\{\mathrm{erf}\,\frac{z-t}{\xi} + \mathrm{erf}\,\frac{z+t}{\xi}\right\} dt, \tag{35}$$

where the constant $c = -(8/3)F(0)$. The computation was checked by confirming that $\partial f_2/\partial z \to 0$ for large z.

Equations (34), (35) are needed for H70b's viscous drag correction

$$\begin{aligned} F_2 &= \frac{3}{8}\int_0^\infty \left\{f_2(1,z)^2 - f_2(0,z)^2\right\} dz + \int_{-1}^1 f_2(x,0) d\mu_2 + \\ &\quad + \frac{1}{16}\int_0^\infty\int_{-1}^1 \left(\frac{\partial f_2}{\partial z}\right)^2 d\mu_2 dz + O(R^{-1/3}) \\ &= \int_{-1}^1 f_2(x,0)\frac{9\mu_2^2 - 1}{8} d\mu_2 + \int_0^\infty\int_{-1}^1 \left(\frac{\partial f_2}{\partial z}\right)^2 \frac{9\mu_2^2 - 5}{64} d\mu_2 dz + O(R^{-1/3}), \end{aligned} \tag{36}$$

in which all the integrations were done numerically with NAG Gaussian routines, with 32, 64 and 128 grid points in each direction to check the convergence. Integrating beyond $z = 20$ appeared to give no useful additional accuracy.

***** Figure 5 near here *****

The results are shown in Figure 5, which should be compared with Figure 4. The finite-s correction of (4) was small but useful; without it F_1 in Figure 5 would have been constant

at 2.211, but with it the curve rises slightly as d decreases past about 6, to a maximum near $d = 3.4$, and then falls. The rise is rather less than that of YP, but it is there. However F_2 behaves very differently in Figures 4 and 5 for small d; (4) is evidently good enough for the second bubble only if $d > 4$. To pursue the present form of the theory to smaller values of d would require not only a better approximation to ΔC_D than (4), but also better approximations in various equations in Sections 2, 3 and 5. They are beyond the scope of this paper.

Figure 5 confirms the result (YP) that $F_2 \to 2.211$ as $d \to \infty$ for fixed large R. The numerical integration of (36) also confirmed the result (H70) that $F_2 \to 4.345$ as $R \to \infty$ for fixed large d, but as YP said, the former limiting case is of more practical use than the latter.

6 The speed of the second bubble

KM pointed out that as the second bubble rises in the wake of the first, its upward velocity is increased above what would be predicted from its calculated drag coefficient. If the downstream distance $X \gg aR$ and $m = O(a)$, the upward velocity u_X due to the first bubble is

$$u_X = U(a/X)^3 + 3UX^{-1}\exp(-Um^2/4\nu X), \tag{37}$$

(Rosenhead 1963, KM). KM suggested approximating to the effect of the second bubble rising in this fluid by averaging u_X over the projected area of that bubble, i.e. by taking that bubble to have an additional upward velocity $\overline{u}$ given by

$$\overline{u} = \int_0^a m u_X \, dm \Big/ \int_0^a m \, dm = U(a/X)^3 + 24UR^{-1}(1 - e^{-8Ra/X}), \tag{38}$$

$$\sim U(a/X)^3 + 24UR^{-1}, \tag{39}$$

when one uses (37). This result, proved by KM if $X/a \gg R$, is still true if $X/a > o(1)$, because the second term in (38) can be estimated from the theory of Section 4 above as

$$u_{wake} = \frac{8}{R^{1/2}} \int_0^\infty u \, dz \text{where } u = -\frac{4Ua^2}{R^{1/2}} \int_z^\infty \Omega(w, z') \, dz', \tag{40}$$

$$\therefore \frac{\partial u_{wake}}{\partial w} = 0, \tag{41}$$

by (29). The dominant term for us is thus $\overline{u} = O(R^{-1}U)$, which gives a smaller contribution at large R than has already been ignored above, but because $R \leq 112$ in the experiments

of KM it cannot be ignored there. Unfortunately the bubbles observed by KM were rising beneath many previous bubbles, not just one, and the series $\sum_{j=1}^{j=n}(1 - \mathrm{e}^{-8Rs/j})$ diverges logarithmically as the number of bubbles $n \to \infty$. Physically, that means that a full theory for the KM experiments would require knowledge of n, or failing that, careful consideration of wall effects and of the effects of the bottom of the tank and of the free surface at moderate values of R. It will not be attempted here.

7 Conclusions

The question investigated in this paper was "Why is the first approximation (for large R and at least moderately large d) so bad?" The answer seems to be "Because one can ignore viscous diffusion in the wake between bubbles only if the Reynolds number is impossibly high, and because a line of three or more bubbles differs in important ways from a line of two." The major discrepancy between H70b and YP was removed in Section 4 which obtains the major effect of viscosity in the wake between bubbles. Lesser but still important improvements were made in Section 3 by including the $R^{-1/6}$ order velocity perturbations near the rear stagnation point on the first bubble, which affect the drag on that bubble very little but on the second bubble rather more, and by including the finite-s correction described in Section 1. The other finite-s corrections mentioned at the end of Section 5 would be less important, except for bubbles very close together.

Acknowledgements

I wish to thank the Victoria University of Wellington for a period of research and study leave, the Department of Earth Sciences, Cambridge, for facilities and hospitality, Wolfson College Cambridge for a visiting fellowship during which this paper was written, Professor Prosperetti for arranging a visit to Johns Hopkins University, and Dr Yuan for the computer files enabling me to prepare Figures 1 and 4 (which are redrawn after YP Figures 4 and 3.)

References

Bateman Manuscript Project 1954 *Tables of integral transforms*, vol. II. McGraw-Hill, New York.

Blanco, A. & Magnaudet, J. 1995 The structure of the axisymmetric high-Reynolds number flow around an ellipsoidal bubble of fixed shape. *Phys. Fluids* **7**, 1265–1274.

Brabston, D.C. & Keller, H.B. 1975 Viscous flows past spherical gas bubbles. *J. Fluid Mech.* **69**, 179–189.

Carslaw, H.S. and Jaeger, J.C. 1959 *Conduction of heat in solids.* Oxford University Press, Oxford and New York.

Dandy, D.S. & Leal, L.G. 1986 Boundary layer separation from a smooth slip surface. *Phys. Fluids* **29**, 1360–1366.

Duineveld, P.C. 1995 The rise velocity and shape of bubbles in pure water at high Reynolds number. *J. Fluid Mech.* **292**, 325–332.

Gradshteyn, I.S. & Ryzhik, I.M. 1980 *Tables of Integrals, Series and Products.* Academic Press, New York.

Harper, J.F. 1970a Viscous drag in steady potential flow past a bubble. *Chem. engng Sci.* **25**, 342–343.

Harper, J.F. 1971 Errata. *Chem. engng Sci.* **26**, 501.

Harper, J.F. 1970b On bubbles rising in line at large Reynolds numbers. *J. Fluid Mech.* **41**, 751–758.

Harper, J.F. 1972 The motion of bubbles and drops through liquids. *Adv. appl. Mech.* **12**, 59–129.

Harper, J.F. 1983 Axisymmetric Stokes flow images in spherical free surfaces with applications to rising bubbles. *J. Austral. Math. Soc. Ser. B* **25**, 217-231

Harper, J.F. & Moore, D.W. 1968 The motion of a spherical liquid drop at high Reynolds numbers. *J. Fluid Mech.* **32**, 367–391.

Katz, J. & Meneveau, C. 1996 Wake-induced relative motion of bubbles rising in line. *Int. J. Multiphase Flow* **22** 239–258.

Lerner, L. & Harper, J.F. 1991 Stokes flow past a pair of stagnant-cap bubbles. *J. Fluid Mech.* **232**, 167–190.

Levich, V.G. 1949 Motion of gaseous bubbles with high Reynolds numbers. (In Russian).

Zh. Eksp. Teor. Fiz. **19**, 18–24.

Magnaudet, J., Rivero, M. & Fabre, J. 1995 Accelerated flows past a rigid sphere or a spherical bubble. Part 1. Steady straining flow. *J. Fluid Mech.* **284**, 97–135.

Maxworthy, T., Gnann, C., Kürten, M. & Durst, F. 1996 Experiments on the rise of air bubbles in clean viscous liquids. *J. Fluid Mech.* **321**, 421–441.

Moore, D.W. 1963 The boundary layer on a spherical gas bubble. *J. Fluid Mech.* **16**, 161–176.

Moore, D.W. 1965 The velocity of rise of distorted gas bubbles in a liquid of small viscosity. *J. Fluid Mech.* **23**, 749–766.

NAG 1995 *Fortran Library Manual, Mark 17.* Numerical Algorithms Group, Oxford.

Rosenhead, L. (ed.) 1963 *Laminar Boundary Layers*, Oxford University Press, London and New York.

Ryskin, G. & Leal, L.G. 1984a Numerical solution of free-boundary problems in fluid mechanics. Part 1. The finite-difference technique. *J. Fluid Mech.* **148**, 1–17.

Ryskin, G. & Leal, L.G. 1984b Numerical solution of free-boundary problems in fluid mechanics. Part 2. Buoyancy-driven motion of a gas bubble through a quiescent liquid. *J. Fluid Mech.* **148**, 19–35.

Yuan, H. & Prosperetti, A. 1994 On the in-line motion of two spherical bubbles in a viscous fluid. *J. Fluid Mech.* **278**, 325–349.

Figure Captions

FIGURE 1. Vorticity distributions across the wake after YP (unmarked curves) for $R = 100$ (dotted), $R = 200$ (dashed) and $R = 500$ (solid curves), and according to H70b (curves marked $\times$) for the same R values. Curves (c) are for 0.12 radii below the bottom of the upper bubble, (b) for halfway between the bubbles, and (a) for 0.12 radii above the top of the lower bubble.

FIGURE 2. Curves marked $\times$: vorticity distributions across the wake according to (31), *ignoring* the second-order term Ω_2 of (27). Other details as for Figure 1.

FIGURE 3. Curves marked $\times$: vorticity distributions across the wake according to (31), *including* the second-order term Ω_2 of (27). Other details as for Figure 1.

FIGURE 4. Correction factors F_1, F_2 after YP as a function of that paper's centre-to-centre separation d, giving the viscous drag for several values of the Reynolds number R. Solid lines are for the upper bubble (F_1); dashed lines are for the lower bubble (F_2). $\triangle$, $R = 200$; $\square$, $R = 100$; $\bigcirc$, $R = 50$.

FIGURE 5. Correction factors F_1, F_2 found herein as a function of this paper's centre-to-centre separation da, giving the viscous drag for several values of the Reynolds number R. Solid lines are for the upper bubble (F_1); dashed lines are for the lower bubble (F_2), according to both this work and H70b. $\triangle$, $R = 200$; $\square$, $R = 100$; $\bigcirc$, $R = 50$.

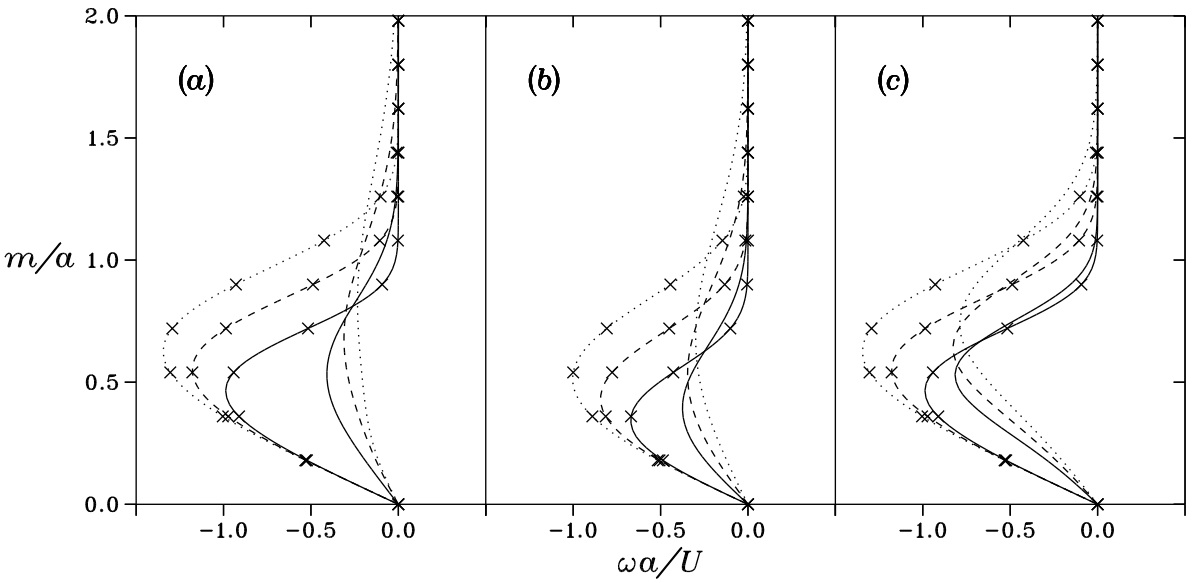

FIGURE 1. Vorticity distributions across the wake after YP (unmarked curves) for $R = 100$ (dotted), $R = 200$ (dashed) and $R = 500$ (solid curves), and according to H70b (curves marked $\times$) for the same R values. Curves (c) are for 0.12 radii below the bottom of the upper bubble, (b) for halfway between the bubbles, and (a) for 0.12 radii above the top of the lower bubble.

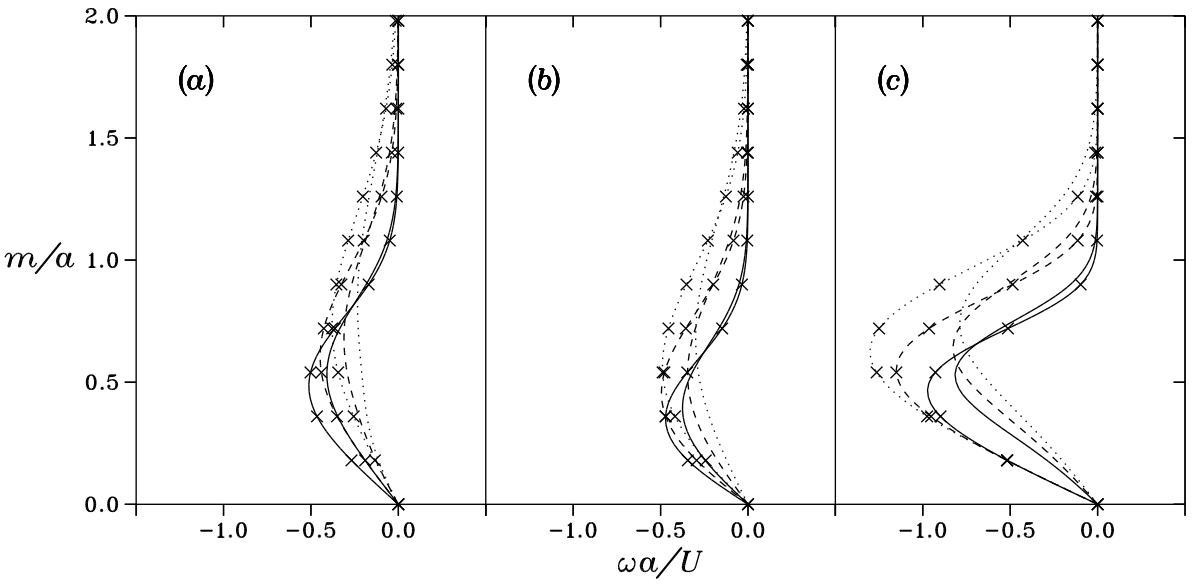

FIGURE 2. Curves marked ×: vorticity distributions across the wake according to (31), *ignoring* the second-order term Ω_2 of (27). Other details as for Figure 1.

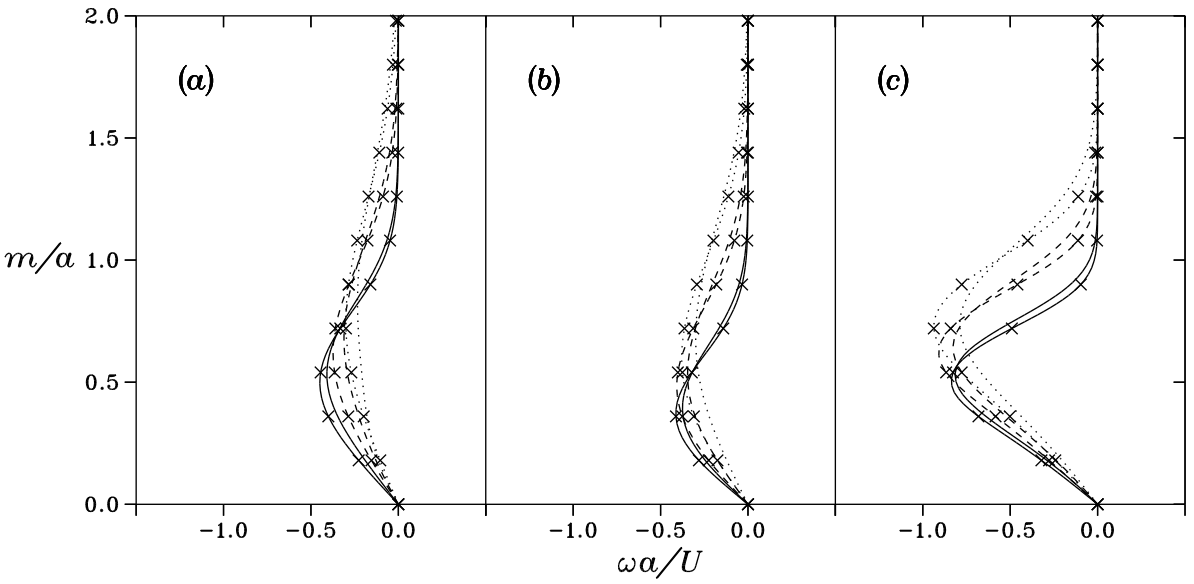

FIGURE 3. Curves marked ×: vorticity distributions across the wake according to (31), *including* the second-order term Ω_2 of (27). Other details as for Figure 1.

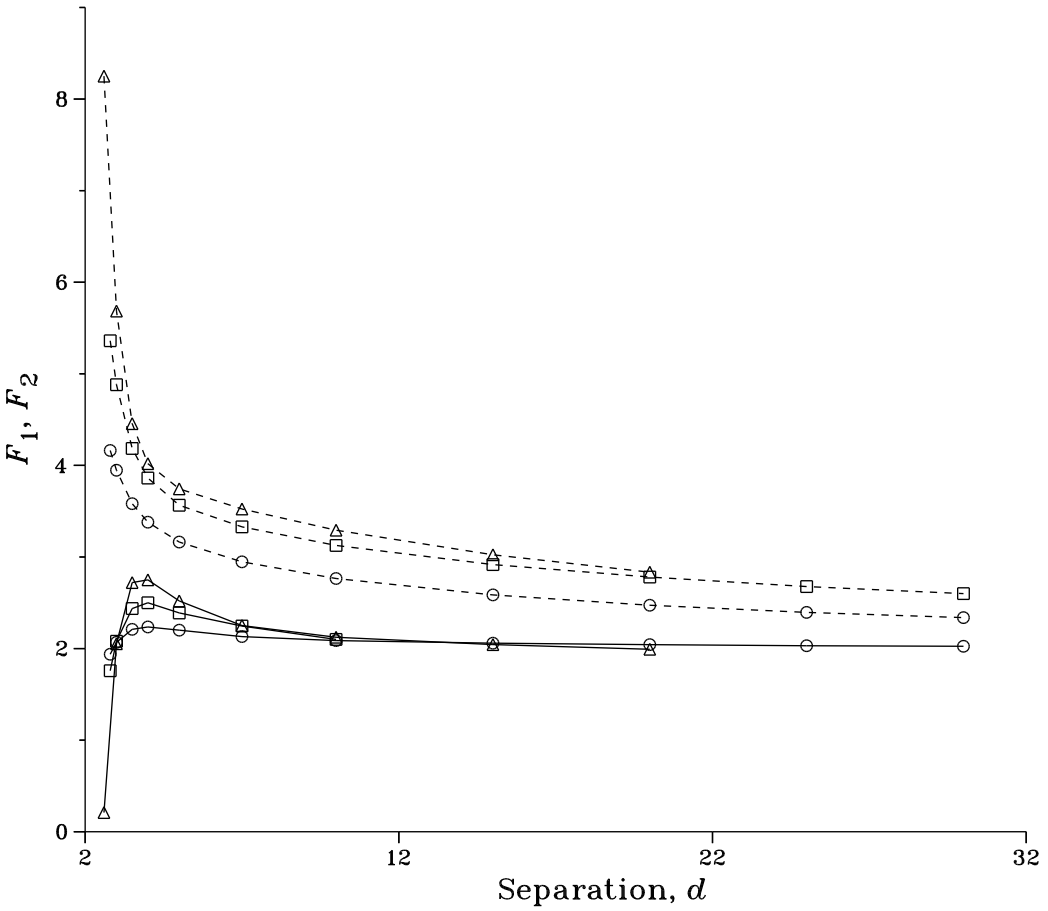

FIGURE 4. Correction factors F_1, F_2 after YP as a function of that paper's centre-to-centre separation d, giving the viscous drag for several values of the Reynolds number R. Solid lines are for the upper bubble (F_1); dashed lines are for the lower bubble (F_2). $\triangle$, $R = 200$; $\square$, $R = 100$; $\bigcirc$, $R = 50$.

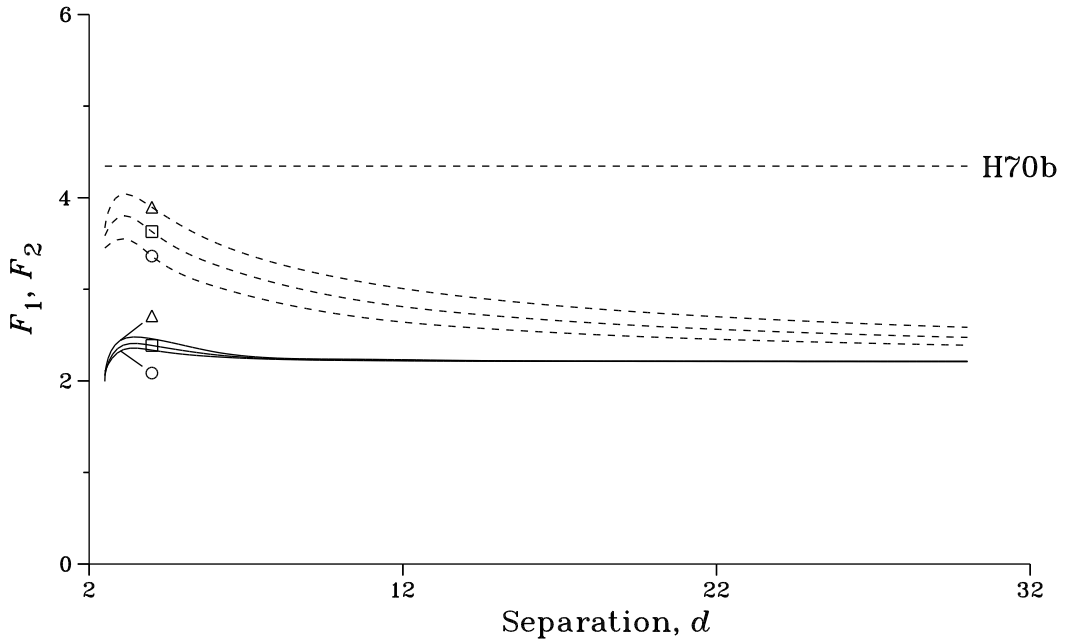

FIGURE 5. Correction factors F_1, F_2 found herein as a function of this paper's centre-to-centre separation da, giving the viscous drag for several values of the Reynolds number R. Solid lines are for the upper bubble (F_1); dashed lines are for the lower bubble (F_2), according to both this work and H70b. $\triangle$, $R = 200$; $\square$, $R = 100$; $\bigcirc$, $R = 50$.